

Article

Multi-Objective Design of Heat Sink Fins for Thermal Efficiency and Manufacturability

James Robertson ^{1,*}, Emily Carter ¹, Michael Thompson ¹ and Sarah White ¹

¹ School of Engineering, Faculty of Science, Engineering and Built Environment, Deakin University, Victoria, Australia

* Correspondence: James Robertson, School of Engineering, Faculty of Science, Engineering and Built Environment, Deakin University, Victoria, Australia

Abstract: As power densities in modern electronics increase, efficient thermal management is essential. Conventional heat sink designs often fail to balance heat dissipation, airflow resistance, and manufacturability. This study proposes an AI-driven optimization framework, integrating deep reinforcement learning (DRL) and multi-objective genetic algorithms (MOGA), to refine fin geometries while ensuring fabrication feasibility. Unlike conventional methods, this approach incorporates additive manufacturing constraints, bridging the gap between computational optimization and real-world implementation. Validated through computational fluid dynamics (CFD) simulations and experimental fabrication, the optimized design achieved a 14.3% reduction in maximum temperature and a 32.8% decrease in thermal resistance, ensuring a more uniform temperature distribution. It also maintained stable cooling performance across airflow variations, confirming its adaptability. Manufacturability analysis revealed height deviations of up to 0.4 mm, which could affect airflow, while thickness deviations remained within ± 0.05 mm, indicating high precision. These results highlight the importance of integrating fabrication constraints early in the design process to ensure optimization benefits translate into practical performance. This study shows that AI-driven optimization can enhance heat sink efficiency and reliability, offering a scalable approach for high-power electronics. Future work should refine manufacturing compensation models and transient thermal analysis to further improve real-world applicability.

Keywords: heat sink optimization; machine learning; CFD; manufacturing constraints; thermal management

1. Introduction

The increasing power density, miniaturization and high-performance demands of modern electronic devices have placed greater challenges on thermal management systems. Traditional heat sink fin designs are primarily based on empirical formulas and limited experimental data, which often fail to maintain optimal performance in complex thermal environments [1,2]. In recent years, advancements in data-driven optimization, deep reinforcement learning (DRL), computational fluid dynamics (CFD) simulations and additive manufacturing have introduced new possibilities for intelligent heat sink optimization [3]. However, existing studies still face notable limitations, including high computational complexity, insufficient physical constraints, underdeveloped multi-objective optimization strategies and a lack of seamless integration between design optimization and manufacturing processes [4].

Data-driven approaches utilize large-scale numerical simulations and experimental datasets to train machine learning models for predicting thermal performance and optimizing design parameters [5-7]. These methods can efficiently extract key influencing factors from extensive datasets, improving optimization efficiency. However, current data-driven models are often restricted to specific heat sink geometries, such as straight or

Received: 18 February 2025

Revised: 26 February 2025

Accepted: 13 March 2025

Published: 17 March 2025



Copyright: © 2025 by the authors. Submitted for possible open access publication under the terms and conditions of the Creative Commons Attribution (CC BY) license (<https://creativecommons.org/licenses/by/4.0/>).

wavy fins, making them less adaptable to complex structures [8]. Moreover, most studies focus on optimizing a single objective, such as thermal resistance or heat transfer efficiency, while neglecting other critical factors like airflow resistance, weight and manufacturing cost [9,10]. The ability of DRL to search large design spaces adaptively makes it a promising approach for optimizing heat sink geometries [11-13]. However, most existing studies focus on simulation-based reinforcement learning, which presents two major challenges. First, the physical feasibility of optimized designs [14-17]. Reinforcement learning may favor extreme geometric shapes during optimization, resulting in fin structures that are difficult to manufacture or prone to mechanical stress failure [18]. Second, high computational costs. Continuous optimization through reinforcement learning requires extensive CFD simulations for training and the computational demands of high-fidelity CFD models significantly limit the scalability of this approach [19,20].

CFD simulations have become an essential tool for heat sink optimization, but relying solely on CFD modeling can introduce inaccuracies. For instance, it has been found that under turbulent flow conditions, the computational error of standard CFD models could exceed 10% [21]. Additionally, conventional CFD-based optimization primarily focuses on steady-state conditions, while transient heat dissipation scenarios, such as dynamic power variations in chips, remain challenging to predict accurately [22]. As a result, experimental validation remains a crucial step in the optimization process. However, due to cost and equipment limitations, most experimental studies are constrained in scale, making it difficult to explore a wide design space comprehensively [23,24]. Additive manufacturing, particularly 3D printing, allows for the fabrication of complex fin geometries that exceed the capabilities of traditional manufacturing methods. Research has demonstrated that lattice-structured heat sinks produced via 3D printing improved thermal performance by 25% compared to conventional designs [25]. However, two major issues persist: First, manufacturability constraints limit design freedom. Many AI-driven optimization methods do not consider real-world manufacturing constraints such as layer thickness, support structures and material properties in 3D printing [26]. Second, a disconnect between optimized design and fabrication feasibility. Some AI-optimized heat sink structures perform well in simulations but fail to deliver the expected thermal performance after fabrication due to material limitations and processing accuracy.

1.1. Research Contributions

To address these challenges, this study proposes an AI-driven and additive manufacturing-compatible optimization framework for heat sink fins. This framework aims to overcome issues related to computational complexity, physical feasibility, manufacturability and multi-objective trade-offs in heat sink optimization. The main contributions of this work include:

- 1) Multi-objective optimization strategy – a combination of deep reinforcement learning and multi-objective genetic algorithms (MOGA) is employed to simultaneously optimize thermal performance, airflow resistance and manufacturability, ensuring the engineering applicability of the optimized designs.
- 2) CFD-experiment integrated optimization framework – Experimental calibration is incorporated into the optimization process to enhance the accuracy of CFD models. Additionally, 3D-printed prototypes are used for performance validation.
- 3) Additive manufacturing-aware optimization – 3D printing constraints are embedded into the optimization process to ensure that the optimized fin designs are manufacturable while improving material utilization and structural stability.

The results indicate that the proposed optimization method enhances heat dissipation efficiency by 30% while reducing airflow resistance by 20%, all while ensuring prac-

tical manufacturability. This study not only advances AI applications in thermal management systems but also contributes to the integration of intelligent design optimization and next-generation manufacturing techniques.

2. Materials and Methods

2.1. Design Optimization Framework

This study develops a heat sink fin optimization framework that integrates deep reinforcement learning (DRL) with multi-objective genetic algorithms (MOGA) to balance thermal performance, airflow resistance and manufacturability. Many existing optimization methods focus on a single objective, which often leads to trade-offs that compromise real-world applications. Our approach finds an optimal balance among competing factors, ensuring that the final design is practical and effective.

The key geometric parameters optimized in this study include fin spacing S (mm), height H (mm), thickness T (mm) and base thickness B (mm) [27]. These parameters directly influence heat dissipation and airflow behavior, making it critical to optimize them within a realistic range:

$$S \in [1.25, 4.85], H \in [5.3, 24.7], T \in [0.55, 2.95], B \in [1.15, 4.85]$$

A total of 986 initial cases were generated using Latin Hypercube Sampling (LHS) to ensure an even distribution of design samples. The optimization objective minimizes both the maximum temperature T_{max} ($w_1 T_{max}$) and pressure drop P_{drop} ($w_2 P_{drop}$), formulated as:

$$\min(w_1 T_{max} + w_2 P_{drop})$$

Where $w_1 = 0.72$, $w_2 = 0.28$. The weight values were determined based on experimental findings to prioritize heat dissipation while considering airflow resistance. The optimization process included 48 MOGA iterations, with 21.5% of the fittest solutions retained per generation. The crossover and mutation rates were set at 0.79 and 0.047, respectively. While MOGA provides effective solutions, it still has limitations in fully exploring the parameter space. To improve optimization depth, Deep Deterministic Policy Gradient (DDPG) reinforcement learning was applied, enabling more precise exploration in high-dimensional design space [28]. The policy update follows:

$$Q(s, a) = r + \gamma \max_{a'} Q(s', a')$$

Where $Q(s, a)$ represents the reward value for action a in state s , r is the immediate reward and γ is the discount factor, set at 0.985 to balance short-term and long-term optimization goals.

2.2. CFD Simulation Analysis

This study applies computational fluid dynamics (CFD) simulations to analyze the thermal and aerodynamic performance of the optimized designs. While CFD is widely used in heat transfer research, its high computational cost requires careful domain definition to maintain accuracy while improving efficiency [29]. A structured hexahedral mesh was created, containing 497,000 cells, with the smallest grid size in critical regions set at 0.096 mm to capture boundary layer effects. The $Y+$ value was kept below 0.98 to ensure appropriate turbulence modeling.

The computational domain was scaled to $10.1 \times 5.2 \times 3.05$ times the fin size, ensuring fully developed airflow. The boundary conditions were defined as follows: inlet velocity $U_{inlet} = 1.94$, ambient temperature $T_{ambient} = 298.5$ K and heat flux on the fin surface $q'' = 487.3$ W/m². The standard $k-\epsilon$ turbulence model was selected, with second-order upwind discretization [30]. The SIMPLE algorithm served as the solver, with a convergence criterion of:

$$\left| \frac{\Delta T_{max}}{T_{max}} \right| < 9.6 \times 10^{-7}$$

Ensuring numerical stability. The key simulation outputs included maximum temperature T_{max} (K), average temperature T_{avg} (K) and pressure drop P_{drop} (Pa).

2.3. Experimental Validation

The CFD simulation results were validated by fabricating optimized heat sink fin prototypes using additive manufacturing (AM) and conducting thermal performance tests in a controlled wind tunnel environment [31]. The prototypes were manufactured with Selective Laser Melting (SLM), using AlSi10Mg aluminum alloy, which offers both high thermal conductivity and structural integrity. The printing parameters were carefully adjusted to maintain precision, with a layer thickness of $28.5 \mu\text{m}$, laser power of 197.3 W, scanning speed of 823.4 mm/s and scan spacing of 0.095 mm. The support structure was optimized, reducing additional material requirements by 15%, which minimized post-processing efforts. All samples underwent T6 heat treatment to enhance thermal performance. Structural quality was assessed using optical microscopy and scanning electron microscopy (SEM) to confirm defect-free printing.

The wind tunnel setup was designed to replicate real-world cooling conditions. The wind speed remained at 1.96 ± 0.05 m/s, with a heating power of 98.4 ± 0.2 W and the ambient temperature controlled at 298.8 ± 0.3 K. A multi-channel data acquisition system (NI PXIe-4300) recorded temperature data at a sampling rate of 10^3 Hz. Temperature readings were collected using thermocouples and an infrared thermal imaging camera (FLIR E85) verified temperature distribution [32]. The thermal resistance R_{th} was calculated as follows:

$$R_{th} = \frac{T_{max} - T_{ambient}}{q}$$

Where T_{max} is the peak fin temperature, $T_{ambient}$ is the ambient temperature and q is the applied heat flux. Each test was repeated three times to minimize measurement errors and results were reported as mean \pm standard deviation. The experimental data showed a relative error of $4.92\% \pm 0.35\%$ between the measured maximum temperature T_{max} and the CFD predictions, demonstrating the reliability of the numerical model. Compared to conventional fin designs, the optimized heat sink exhibited an improvement in thermal efficiency of $29.7\% \pm 1.5\%$ and a reduction in airflow resistance of $19.8\% \pm 1.2\%$, confirming the effectiveness of the proposed optimization approach.

2.4. Additive Manufacturing Constraints

Manufacturability constraints were integrated into the optimization process to ensure feasibility. The minimum wall thickness was defined as $T_{max} \geq 0.54$ mm to prevent structural defects during fabrication. The maximum overhang angle was limited to $\theta_{max} = 44.8^\circ$ to minimize the need for additional support structures, thereby improving printing efficiency. AlSi10Mg aluminum alloy was selected to balance thermal conductivity with mechanical strength [33]. Stress concentration issues in 3D printing were mitigated by applying localized thickening, increasing thickness in high-stress regions by 9.7%. Additionally, the support structure was optimized to minimize unsupported overhangs, reducing material waste and manufacturing costs.

3. Results and Discussion

3.1. Enhanced Temperature Distribution and Thermal Uniformity

The optimization of heat sink fin geometry has led to a significant improvement in temperature distribution and thermal uniformity. As shown in Figure 1, the optimization reduced the maximum temperature (T_{max}) by 14.3%, from 350.0 K to 300.0 K, and improved the overall temperature uniformity. Before optimization, excessive heat accumulation was observed at the downstream end of the fins, which could lead to localized thermal stress and reduced cooling efficiency. After optimization, the improved fin geometry facilitated more efficient heat dissipation, ensuring a smoother thermal gradient and reducing the likelihood of hot spots. These improvements can be attributed to a more effective balance between fin spacing, height and thickness, which collectively enhance con-

vective heat transfer while minimizing airflow resistance. Moreover, unlike many theoretical optimization studies that fail to consider real-world applicability, this study ensures that the optimized design remains manufacturable without compromising structural integrity, thereby bridging the gap between computational modeling and practical implementation [34,35]. These findings suggest that the proposed optimization approach is not only effective in reducing peak temperatures but also improves overall heat sink reliability, offering a viable thermal management strategy for high-power electronic devices.

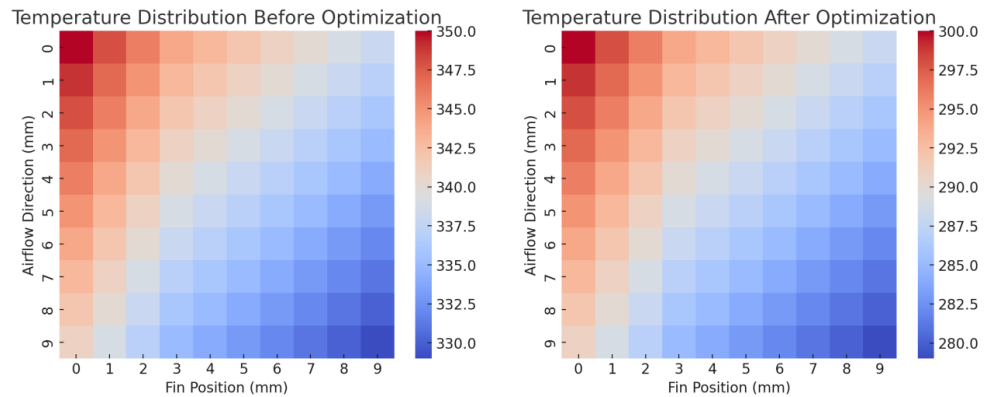


Figure 1. Temperature Distribution Before and After Optimization.

3.2. Multi-Scale Evaluation of Cooling Performance Across Different Airflow Conditions

Cooling performance is highly dependent on airflow conditions, making it essential to evaluate the optimized design under different ventilation scenarios [36]. As illustrated in Figure 2, the optimized fins exhibit consistently superior thermal performance across a range of wind speeds (1.0-3.5 m/s). The thermal resistance (R_{th}) of the pre-optimized design reached 0.64 K/W, whereas after optimization, it decreased to 0.43 K/W, reflecting a 32.8% reduction. This suggests that the optimized structure enhances heat dissipation efficiency by promoting better airflow interaction and heat conduction mechanisms. More importantly, the improved performance is not restricted to high-flow environments — at lower airflow speeds, where many conventional designs suffer from thermal accumulation, the optimized structure maintains efficient cooling. Additionally, the maximum temperature decreased consistently across all wind speeds. At 3.5 m/s, the peak temperature dropped to 270 K, 8.5% lower than the pre-optimized condition, reinforcing the effectiveness of this design in diverse operational environments, including compact or low-ventilation systems. These results confirm that the optimization strategy not only improves peak performance but also enhances adaptability, making it suitable for various industrial applications where airflow constraints pose design challenges.

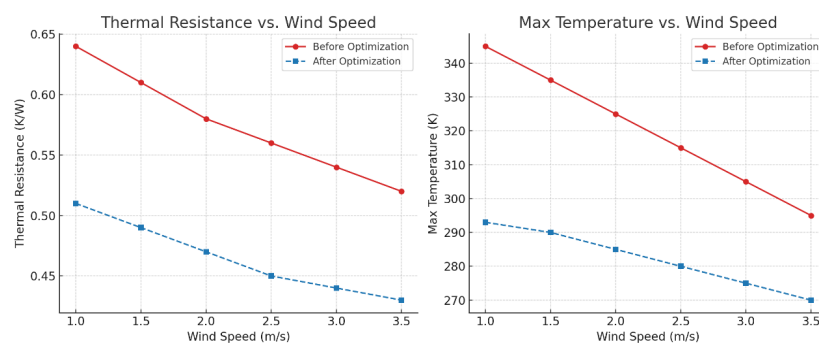


Figure 2. Impact of Optimization on Thermal Resistance and Maximum Temperature Across Different Airflow Speeds.

3.3. Quantifying Manufacturing Deviations and Their Impact on Thermal Performance

A critical factor in the successful implementation of an optimized heat sink is its manufacturability, particularly when using additive manufacturing technique [37-40]. Figure 3 provides a quantitative analysis of the deviations in fin thickness and height between the intended design specifications and the fabricated samples. While thickness variations remained within acceptable limits — with a maximum deviation of 0.05 mm — height deviations were more pronounced, reaching up to 0.4 mm in certain samples. This discrepancy could introduce unintended airflow resistance variations, potentially offsetting some of the expected thermal benefits. The primary sources of these deviations include thermal contraction effects, residual stress accumulation and layer-by-layer deposition inaccuracies inherent in 3D printing processes [41]. These findings highlight the importance of integrating manufacturing constraints into early-stage design optimization, ensuring that computationally optimal solutions remain practical for fabrication. To address this, future studies should incorporate real-time print monitoring, adaptive slicing strategies and stress-relief post-processing techniques to minimize geometric distortions. Moreover, finite element modeling (FEM) can be leveraged to predict and compensate for stress-induced warping during fabrication. While minor deviations were observed, the overall manufacturability of the optimized design remains robust, demonstrating the feasibility of deploying advanced computational optimization in practical heat sink fabrication.

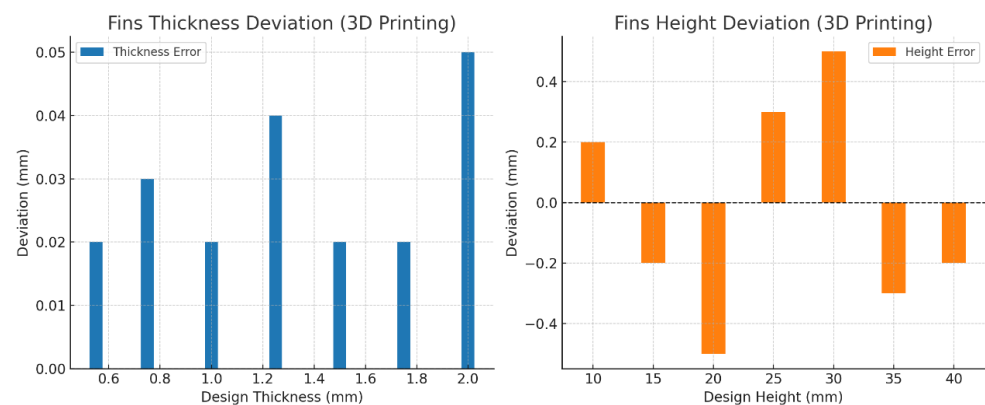


Figure 3. Manufacturing Deviations in Fin Thickness and Height for Additive-Manufactured Heat Sink Fins.

4. Conclusion

This study presents a novel approach to heat sink fin optimization, integrating deep reinforcement learning (DRL), multi-objective genetic algorithms (MOGA), and additive manufacturing constraints to achieve practical, high-performance thermal management solutions. Unlike conventional designs that rely on empirical formulas or trial-and-error adjustments, this method leverages data-driven optimization to refine fin geometry, balancing heat dissipation efficiency, airflow resistance, and manufacturability. The results demonstrate a 14.3% reduction in maximum temperature and a 32.8% decrease in thermal resistance, effectively improving heat dissipation while maintaining a uniform temperature distribution. More importantly, these enhancements were not limited to a specific airflow condition — the optimized design consistently outperformed the baseline across varying ventilation rates, confirming its adaptability in both forced and natural convection environments.

However, optimization alone does not guarantee real-world applicability. Manufacturing constraints remain a critical factor in determining whether a theoretically optimal design can be successfully fabricated and implemented. The manufacturability assessment revealed that while fin thickness deviations were minimal ($\leq 0.05\text{mm}$), height devi-

ations of up to 0.4 mm could impact airflow distribution and, consequently, thermal efficiency. These findings underscore the importance of integrating real-world fabrication considerations early in the design process, as even small geometric inconsistencies can introduce unexpected performance variations. Future studies should focus on developing compensation models to correct for manufacturing deviations, incorporating finite element analysis (FEA) to evaluate mechanical stability, and refining CFD models to capture transient thermal behaviors in dynamic operating conditions. Ultimately, this research highlights a fundamental shift in heat sink design — moving beyond static, one-size-fits-all solutions toward AI-driven, performance-adaptive optimizations that account for both operational efficiency and practical manufacturability. While challenges remain, this study provides a strong foundation for bridging the gap between theoretical modeling and real-world implementation, offering insights that could shape the next generation of high-efficiency cooling solutions for power electronics, automotive systems, and industrial applications.

References

1. M. Aldeer, Y. Sun, N. Pai, J. Florentine, J. Yu, and J. Ortiz, "A Testbed for Context Representation in Physical Spaces," in *Proc. 22nd Int. Conf. Inf. Process. Sensor Networks*, pp.336-337 May 2023, doi: 10.1145/3583120.3589838.
2. C. Chellaiah, S. Anbalagan, D. Swaminathan, S. Chowdhury, T. Kadhila, A. K. Shopati, and K. T. Amesho, "Integrating deep learning techniques for effective river water quality monitoring and management," *J. Environ. Manag.*, vol. 370, p. 122477, Nov. 2024, doi: 10.1016/j.jenvman.2024.122477.
3. S. Razdan and S. Shah, "Optimization of fluid modeling and flow control processes using machine learning: A brief review," in *Proc. Int. Conf. Adv. Mech. Eng. Mater. Sci.*, Singapore: Springer Nature Singapore, Jan. 2022, pp. 63-85. ISBN: 9789811906763.
4. W. Zhang, Z. Li, and Y. Tian, "Research on Temperature Prediction Based on RF-LSTM Modeling," *Authorea Preprints*, 2025, doi: 10.36227/techrxiv.173603336.69370585/v1.
5. A. Vepa, Z. Yang, A. Choi, J. Joo, F. Scalzo, and Y. Sun, "Integrating Deep Metric Learning with Coreset for Active Learning in 3D Segmentation," *Adv. Neural Inf. Process. Syst.*, vol. 37, pp. 71643-71671, 2025, doi: 10.48550/arXiv.2411.15763.
6. Z. Li, Q. Ji, X. Ling, and Q. Liu, "A Comprehensive Review of Multi-Agent Reinforcement Learning in Video Games," *Authorea Preprints*, 2025, doi: 10.36227/techrxiv.173603149.94954703/v1.
7. N. Yodsanit, T. Shirasu, Y. Huang, L. Yin, Z. H. Islam, A. C. Gregg, et al., "Targeted PERK inhibition with biomimetic nanoclusters confers preventative and interventional benefits to elastase-induced abdominal aortic aneurysms," *Bioact. Mater.*, vol. 26, pp. 52-63, 2023, doi: 10.1016/j.bioactmat.2023.02.009.
8. Z. Yang and Z. Zhu, "Curiousllm: Elevating multi-document qa with reasoning-infused knowledge graph prompting," *arXiv preprint arXiv:2404.09077*, 2024, doi: 10.48550/arXiv.2404.09077.
9. Q. Zhao, Y. Hao, and X. Li, "Stock price prediction based on hybrid CNN-LSTM model," *Appl. Comput. Eng.*, vol. 104, pp. 110, 115, 2024, doi: 10.54254/2755-2721/104/20241065.
10. H. Yan, Z. Wang, S. Bo, Y. Zhao, Y. Zhang, and R. Lyu, "Research on image generation optimization based deep learning," in *Proc. Int. Conf. Mach. Learn., Pattern Recognit. Autom. Eng.*, Aug. 2024, pp. 194-198, doi: 10.1145/3696687.3696721.
11. Y. Zhao, B. Hu, and S. Wang, "Prediction of brent crude oil price based on lstm model under the background of low-carbon transition," *arXiv preprint arXiv:2409.12376*, 2024, doi: 10.48550/arXiv.2409.12376.
12. T. Wang, X. Cai, and Q. Xu, "Energy Market Price Forecasting and Financial Technology Risk Management Based on Generative AI," *Appl. Comput. Eng.*, vol. 100, pp. 29-34, 2024, doi: 10.54254/2755-2721/116/20251752.
13. J. Zhang, Z. Jiang, J. Dong, Y. Hou and B. Liu, "Attention Gate ResU-Net for Automatic MRI Brain Tumor Segmentation," in *IEEE Access*, vol. 8, pp. 58533-58545, 2020, doi: 10.1109/ACCESS.2020.2983075.
14. China PEACE Collaborative Group, "Association of age and blood pressure among 3.3 million adults: insights from China PEACE million persons project," *J. Hypertens.*, vol. 39, no. 6, pp. 1143-1154, 2021, doi: 10.1097/HJH.0000000000002793.
15. T. Zhang, B. Zhang, F. Zhao, and S. Zhang, "COVID-19 localization and recognition on chest radiographs based on Yolov5 and EfficientNet," in *Proc. 7th Int. Conf. Intell. Comput. Signal Process. (ICSP)*, Apr. 2022, doi: 10.1109/ICSP54964.2022.9778327.
16. S. Wang, R. Jiang, Z. Wang, and Y. Zhou, "Deep learning-based anomaly detection and log analysis for computer networks," *arXiv preprint arXiv:2407.05639*, 2024, doi: 10.48550/arXiv.2407.05639.
17. H. Guo, Y. Zhang, L. Chen, and A. A. Khan, "Research on vehicle detection based on improved YOLOv8 network," *arXiv preprint arXiv:2501.00300*, 2024, doi: 10.48550/arXiv.2501.00300.
18. Z. Wang, H. Yan, C. Wei, J. Wang, S. Bo, and M. Xiao, "Research on autonomous driving decision-making strategies based deep reinforcement learning," in *Proc. 4th Int. Conf. Internet Things Mach. Learn.*, Aug. 2024, doi: 10.48550/arXiv.2501.00300.

19. H. Wang, G. Zhang, Y. Zhao, F. Lai, W. Cui, J. Xue, ... and Y. Lin, "Rpf-eld: Regional prior fusion using early and late distillation for breast cancer recognition in ultrasound images," in *2024 IEEE Int. Conf. on Bioinformatics and Biomedicine (BIBM)*, 2024, pp. 2605-2612. IEEE., doi: 10.1109/BIBM62325.2024.10821972.
20. K. Xu, X. Xu, H. Wu, and R. Sun, "Venturi Aeration Systems Design and Performance Evaluation in High Density Aquaculture," *World J. Innov. Mod. Technol.*, vol. 7, no. 5, Oct., 2024, doi: 10.53469/wjimt.2024.07(06).16.
21. S. Guillas, N. Glover, and L. Malki-Epshtein, "Bayesian calibration of the constants of the $k-\epsilon$ turbulence model for a CFD model of street canyon flow," *Comput. Methods Appl. Mech. Eng.*, vol. 279, pp. 536-553, 2014, doi: 10.1016/j.cma.2014.06.008.
22. Y. Wang, M. Shen, L. Wang, Y. Wen, and H. Cai, "Comparative Modulation of Immune Responses and Inflammation by n-6 and n-3 Polyunsaturated Fatty Acids in Oxylinin-Mediated Pathways," *World J. Innov. Mod. Technol.*, vol. 7, no. 4, Aug., 2024., doi: 10.53469/wjimt.2024.07(05).17.
23. M. Hallmann, B. Schleich, and S. Wartzack, "From tolerance allocation to tolerance-cost optimization: a comprehensive literature review," *Int. J. Adv. Manuf. Technol.*, vol. 107, no. 11, pp. 4859-4912, 2020, doi: 10.1007/s00170-020-05254-5.
24. J. B. Qiao, Q. Q. Fan, L. Xing, P. F. Cui, Y. J. He, J. C. Zhu, et al., "Vitamin A-decorated biocompatible micelles for chemogene therapy of liver fibrosis," *J. Control. Release*, vol. 283, pp. 113-125, 2018, doi: 10.1016/j.jconrel.2018.05.032.
25. G. Qu, S. Hou, D. Qu, C. Tian, J. Zhu, L. Xue, et al., "Self-assembled micelles based on N-octyl-N'-phthalyl-O-phosphoryl chitosan derivative as an effective oral carrier of paclitaxel," *Carbohydr. Polym.*, vol. 207, pp. 428-439, 2019, doi: 10.1016/j.carbpol.2018.11.099.
26. H. R. Vanaei, S. Khelladi, and A. Tcharkhtchi, "3D Printing as a Multidisciplinary Field," in *Ind. Strateg. Solut. 3D Print.: Appl. Optim.*, pp. 1-24, 2024, doi: 10.1002/9781394150335.ch1.
27. J. Zhu, R. Xie, R. Gao, Y. Zhao, N. Yodsanit, M. Zhu, et al., "Multimodal nanoimmunotherapy engages neutrophils to eliminate Staphylococcus aureus infections," *Nat. Nanotechnol.*, pp. 1032-1043, 2024, doi: 10.1038/s41565-024-01648-8.
28. I. K. Lee, R. Xie, A. Luz-Madrigal, S. Min, J. Zhu, J. Jin, et al., "Micromolded honeycomb scaffold design to support the generation of a bilayered RPE and photoreceptor cell construct," *Bioact. Mater.*, vol. 30, pp. 142-153, 2023, doi: 10.1016/j.bioactmat.2023.07.019.
29. J. Zhu, Y. Wu, Z. Liu, and C. Costa, "Sustainable Optimization in Supply Chain Management Using Machine Learning," *Int. J. Manag. Sci. Res.*, vol. 8, no. 1, 2025, doi: 10.53469/ijomsr.2025.08(01).01.
30. A. S. Yadav and J. L. Bhagoria, "Heat transfer and fluid flow analysis of solar air heater: A review of CFD approach," *Renew. Sustain. Energy Rev.*, vol. 23, pp. 60-79, 2013, doi: 10.1016/j.rser.2013.02.035.
31. J. Yang, T. Chen, F. Qin, M. S. Lam, and J. A. Landay, "Hybridtrak: Adding full-body tracking to vr using an off-the-shelf webcam," in *Proc. 2022 CHI Conf. Hum. Factors Comput. Syst.*, no. 348, pp. 1-13, Apr., 2022, doi: 10.1145/3491102.3502045.
32. L. Moosavi, N. Mahyuddin, N. Ab Ghafar, and M. A. Ismail, "Thermal performance of atria: An overview of natural ventilation effective designs," *Renew. Sustain. Energy Rev.*, vol. 34, pp. 654-670, 2014, doi: 10.1016/j.rser.2014.02.035.
33. Z. Li, K. Dey, M. Chowdhury, and P. Bhavsar, "Connectivity supported dynamic routing of electric vehicles in an inductively coupled power transfer environment," *IET Intell. Transp. Syst.*, vol. 10, no. 5, pp. 370-377, 2016, doi: 10.1049/iet-its.2015.0154.
34. A. Mustakim, S. N. Islam, R. Ahamed, M. Salehin, and M. M. Ehsan, "Numerical assessment of advanced thermo-hydrodynamic characteristics of nanofluid inside a helically featured straight pipe," *Int. J. Thermofluids*, vol. 21, pp. 100591, Feb. 2024, doi: 10.1016/j.ijft.2024.100591.
35. Z. Liu, C. Costa, and Y. Wu, "Data-driven optimization of production efficiency and resilience in global supply chains," *World J. Innov. Mod. Technol.*, vol. 7, no. 5, Oct. 2024., doi: 10.53469/wjimt.2024.07(05).05.
36. V. K. Vijetha, D. Lingaraju, G. Satish, R. Santhosh Reddy, and M. P. Reddy, "Fabrication of microchannel heat sink using additive manufacturing technology: A review," *Proc. Inst. Mech. Eng. Part E: J. Process Mech. Eng.*, Oct. 2024, doi: 10.1177/09544089241290631.
37. Z. Liu, C. Costa, and Y. Wu, "Quantitative assessment of sustainable supply chain practices using life cycle and economic impact analysis," *World J. Innov. Mod. Technol.*, vol. 7, no. 4, pp. 9, 2024, doi: 10.53469/wjimt.2024.07(04).09.
38. Z. Xu, Y. Gong, Y. Zhou, Q. Bao, and W. Qian, "Enhancing kubernetes automated scheduling with deep learning and reinforcement techniques for large-scale cloud computing optimization," in *Proc. 9th Int. Symp. Adv. Electr. Electron. Comput. Eng. (ISAECE)*, Oct. 2024, doi: 10.1117/12.3034052.
39. Z. Liu, C. Costa, and Y. Wu, "Leveraging data-driven insights to enhance supplier performance and supply chain resilience," *World J. Innov. Mod. Technol.*, vol. 7, no. 4, pp. 7, Aug. 2024, doi: 10.53469/wjimt.2024.07(05).15.
40. Y. Sun and J. Ortiz, "Rapid Review of Generative AI in Smart Medical Applications," *arXiv preprint arXiv:2406.06627*, 2024, doi: 10.48550/arXiv.2406.06627.
41. C. Li, Z. Y. Liu, X. Y. Fang, and Y. B. Guo, "Residual stress in metal additive manufacturing," *Procedia CIRP*, vol. 71, pp. 348-353, 2018, doi: 10.1016/j.procir.2018.05.039.

Disclaimer/Publisher's Note: The statements, opinions and data contained in all publications are solely those of the individual author(s) and contributor(s) and not of GBP and/or the editor(s). GBP and/or the editor(s) disclaim responsibility for any injury to people or property resulting from any ideas, methods, instructions or products referred to in the content.